

C/O vs. Mg/Si ratios in solar type stars: The HARPS sample[★]

L. Suárez-Andrés^{1,2,3}, G. Israelian^{1,2}, J. I. González Hernández^{1,2}, V. Zh. Adibekyan⁴,
E. Delgado Mena⁴, N. C. Santos^{4,5}, and S. G. Sousa^{4,5}

¹ Instituto de Astrofísica de Canarias, 38205 La Laguna, Tenerife, Spain
e-mail: lsuarez@ing.iac.es

² Departamento de Astrofísica, Universidad de La Laguna (ULL), 38206 La Laguna, Tenerife, Spain

³ Isaac Newton Group of Telescopes, Apartado de Correos 321, 38700 Santa Cruz de la Palma, Spain

⁴ Instituto de Astrofísica e Ciências do Espaço, Universidade do Porto, CAUP, Rua das Estrelas, 4150-762 Porto, Portugal

⁵ Departamento de Física e Astronomia, Faculdade de Ciências, Universidade do Porto, 4169-007 Porto, Portugal

Received 7 March 2017 / Accepted 14 January 2018

ABSTRACT

Aims. We aim to present a detailed study of the magnesium-to-silicon and carbon-to-oxygen ratios (Mg/Si and C/O) and their importance in determining the mineralogy of planetary companions.

Methods. Using 499 solar-like stars from the HARPS sample, we determined C/O and Mg/Si elemental abundance ratios to study the nature of the possible planets formed. We separated the planetary population in low-mass planets ($<30 M_{\odot}$) and high-mass planets ($>30 M_{\odot}$) to test for a possible relation with the mass.

Results. We find a diversity of mineralogical ratios that reveal the different kinds of planetary systems that can be formed, most of them dissimilar to our solar system. The different values of the Mg/Si and C/O can determine different composition of planets formed. We found that 100% of our planetary sample present $C/O < 0.8$. 86% of stars with high-mass companions present $0.8 > C/O > 0.4$, while 14% present C/O values lower than 0.4. Regarding Mg/Si, all stars with low-mass planetary companion showed values between one and two, while 85% of the high-mass companion sample does. The other 15% showed Mg/Si values below one. No stars with planets were found with $Mg/Si > 2$. Planet hosts with low-mass companions present C/O and Mg/Si similar to those found in the Sun, whereas stars with high-mass companions have lower C/O.

Key words. stars: abundances – stars: atmospheres – planetary systems

1. Introduction

The determination of the chemical composition of extrasolar planets has been the subject of numerous studies in recent years. One of the keystones has been the fact that stars hosting giant planets are considered to be metal-rich when compared with single stars (Gonzalez 1997; Santos et al. 2001, 2004; Fischer & Valenti 2005; Gonzalez 2006). Stars hosting low mass planets (those with masses below $30 M_{\odot}$) do not seem to be preferentially metal-rich (e.g. Sousa et al. 2008, 2011a)

Recent studies of chemical abundances in stars with and without planets have shown no important differences in $[X/Fe]$ vs. $[Fe/H]$ trends between the two groups of stars for refractory (González Hernández et al. 2010; Delgado Mena et al. 2010) and volatile elements (Suárez-Andrés et al. 2016, 2017). On the other hand, studies by Haywood (2008, 2009) and Adibekyan et al. (2012a) found evidence of α -elements enhancement in stars with planets.

As both planetesimals and planets are formed within the same environment, their composition is expected to be the same as that of their host star. This assumption might be true for refractory species, but not for the volatile ones (Lodders 2003; Thiabaud et al. 2014). Although this fact does not affect the magnesium-to-silicon ratio (Mg/Si) for rocky planets, it can affect the carbon-to-oxygen ratio (C/O)

Dorn et al. 2015; Thiabaud et al. 2015b). Elemental abundance ratios (C/O and Mg/Si) are important as they govern the distribution and formation of chemical species in the protoplanetary disc.

Variations in C/O can be found among planetary atmospheres and host stars (Madhusudhan et al. 2012; Konopacky et al. 2013; Moses et al. 2013; Brewer et al. 2017) and among planets in the same planetary system. This is due to different parameters (temperature, pressure, etc.) and processes at work during the planet formation stage, including possible migrations of planets from their birthplace (Öberg et al. 2011; Ali-Dib et al. 2014; Madhusudhan et al. 2012; Thiabaud et al. 2015a,b; Brewer et al. 2017)

In the last few years, several studies have tried to understand the formation and evolution of planets using theoretical models. Bond et al. (2010a,b), Carter-Bond et al. (2012) studied planet formation scenarios with different initial composition, but they did not carry out a detailed study of the output volatile species. Elser et al. (2012) tried to study this planet formation model by adding the formation of solids, but they were unable to reproduce some features present in the solar system, such as high Fe on Mercury.

Recently, Thiabaud et al. (2014), Marboeuf et al. (2014) made a complete study, presenting models not only for refractory species, but for volatiles as well. Thiabaud et al. (2015a) presented a complete study, taking into account the accretion of several compounds omitted in previous works such as He, H₂, H₂O, CO, CO₂, CH₃OH, CH₄, NH₃, N₂, and H₂S. Also,

[★]The full Table 1 is only available at the CDS via anonymous ftp to cdsarc.u-strasbg.fr (130.79.128.5) or via <http://cdsarc.u-strasbg.fr/viz-bin/qcat?J+A+614/A84>

they computed the importance of volatile elements in protoplanetary discs and their implications in planetary formation (Thiabaud et al. 2015b). Their models show that the condensation of volatile species as a function of radial distance allows for C/O enrichment in specific parts of the protoplanetary disc of up to four times the solar value. This could lead to the formation of planets that can be enriched in C/O in their envelope up to three times the solar value. Their models are consistent with recent observations of hot-Jupiter atmospheres (Brewer et al. 2017).

The amount of carbides and silicates formed in planets is controlled by the carbon-oxygen ratio (e.g. Bond et al. 2010a)

- if $C/O < 0.8$: Si will form solid SiO_4^{4-} and SiO_2 , serving as seeds for Mg silicates for which the exact composition will be determined by Mg/Si;
- if $C/O > 0.8$: Si will be solid as SiC. Also, graphite and TiC will be formed.

Silicates are an important ingredient in the formation of rocky planets, as they are the most abundant compounds in the mantle and crust of these planets (Morgan & Anders 1980). Silicate distribution is ruled by Mg/Si of the planet host star. Concerning Mg/Si, the principal components could be, as proposed by Bond et al. (2010b):

- if $\text{Mg/Si} < 1$, Mg forms orthopyroxene (MgSiO_3) and the remaining Si forms other minerals, such as feldspar ($\text{CaAl}_2\text{Si}_2\text{O}_8$, $\text{NaAlSi}_3\text{O}_8$) or olivine (Mg_2SiO_4);
- if $1 < \text{Mg/Si} < 2$, Mg is distributed equally between pyroxene and olivine;
- if $\text{Mg/Si} > 2$, Si forms olivine and the remaining Mg forms other oxides like MgO.

Testing and improving planetary formation models is key to future studies of habitability, as these ratios are essential elements in defining the structure of the planet.

In this article we present a study of C/O and Mg/Si in solar-type stars and their implications for possible terrestrial planetary formation.

2. Sample description

The high-resolution spectra analysed in this article were obtained with the HARPS spectrograph at La Silla Observatory (ESO, Chile) during the HARPS GTO, HARPS-2, and HARPS-4 programmes (see Mayor et al. 2003; Lo Curto et al. 2010; Santos et al. 2011, for more information about the programme). The spectra have been used previously in the analysis of stellar parameters, as well as the derivation of precise chemical abundances (see e.g. Sousa et al. 2008, 2011a,b; Adibekyan et al. 2012b; Tsantaki et al. 2013; Bertran de Lis et al. 2015; Suárez-Andrés et al. 2017).

The studied sample is part of the 1111-star sample presented by Adibekyan et al. (2012b) for which the abundance of volatiles were measured (Bertran de Lis et al. 2015; Suárez-Andrés et al. 2017). We limited our metallicity sample for stars with $[\text{Fe}/\text{H}] > -0.6$, which is the lower $[\text{Fe}/\text{H}]$ for the planet-host sample. We studied 499 FGK solar-type stars, with effective temperatures between 5250 K and 6666 K, metallicities from -0.59 to 0.55 dex, and surface gravities from 3.81 to 4.82 dex.

Of 499 stars, 99 are planet hosts¹, whereas the other 400 are single stars (stars with no known planetary companion, also known as comparison stars. We urge the reader to take into account that stars considered as single stars might harbour undetected planets (see Mayor et al. 2011; Faria et al. 2016).

¹ Data from www.exoplanet.eu and the SWEET-CAT catalogue (www.astro.up.pt/resources/sweet-cat/).

Table 1. Sample of C/O and Mg/Si abundances for a set of stars.

Star	T_{eff}	$\log g$	[Fe/H]	C/O	Mg/Si
HD39091	5991	4.40	0.09	0.61 ± 0.11	1.11 ± 0.10
HD82943	5992	4.42	0.28	0.63 ± 0.13	0.99 ± 0.04
HD100508	5384	4.39	0.35	0.54 ± 0.09	0.91 ± 0.01
HD100777	5530	4.31	0.25	0.53 ± 0.04	0.96 ± 0.12
HD102117	5620	4.28	0.26	0.48 ± 0.09	1.07 ± 0.01
HD212708	5644	4.31	0.26	0.51 ± 0.09	1.06 ± 0.07

Notes. The full table is available at CDS.

3. Chemical abundances

To obtain the carbon-to-oxygen (C/O) and magnesium-to-silicon (Mg/Si) elemental abundance ratios we adopted chemical abundances from Adibekyan et al. (2012b); Bertran de Lis et al. (2015) and Suárez-Andrés et al. (2017) for Mg and Si, O, and C, respectively. All these chemical abundances were obtained using the same high-resolution high-quality HARPS spectra and the same stellar parameters, allowing us to obtain precise elemental abundance ratios. For carbon we studied the CH molecular band located at 4300 Å (see Suárez-Andrés et al. 2017), whereas for the other elements atomic features were used. Recent studies of molecular CH features (Suárez-Andrés et al. 2017) have proved that they are as reliable as atomic ones, and provide consistent results.

Although the adopted abundances come from different sources, O, Mg, and Si abundances were obtained following the same procedure (EW method). For the case of C, synthetic fitting was applied, but compared to the EW method results to confirm their validity (see Suárez-Andrés et al. 2017). Errors are significantly lower for Mg and Si (averages 0.06 and 0.04, respectively) than for C and O (average 0.15 for both cases), which affects our final elemental abundance ratio errors.

Adopted solar abundances for all elements are $\log \epsilon(\text{C})_{\odot} = 8.50$ dex (Caffau et al. 2010), $\log \epsilon(\text{O})_{\odot} = 8.71$ (Caffau et al. 2008), $\log \epsilon(\text{Mg})_{\odot} = 7.58$ dex and $\log \epsilon(\text{Si})_{\odot} = 7.55$ (Anders & Grevesse 1989).

4. Elemental abundance ratios

Theoretical studies suggest that C/O and Mg/Si are very important in determining the mineralogy of terrestrial planets. Since the mineralogy of planets is commonly studied in terms of absolute ratios, we use these instead of solar ratios². Elemental abundance ratios were calculated using the following equation

$$A/B = N_A/N_B = 10^{\log \epsilon(A)} / 10^{\log \epsilon(B)}, \quad (1)$$

where $\log \epsilon(A)$ and $\log \epsilon(B)$ are absolute abundances. Errors were estimated by evaluating an increase or decrease in the $\log \epsilon(A) - \log \epsilon(B)$ abundance ratio, due to the relative errors (For more details, see Delgado Mena et al. 2010). Median errors are represented in all figures (0.14 for C/O and 0.06 for Mg/Si). A sample table is shown in Table 1.

4.1. C/O

The C/O in planet-host stars can provide key information about the protoplanetary disc in which the planet was formed. The

² We remind the reader that $C/O \neq [C/O]$. Please see Sect. 6 for more information.

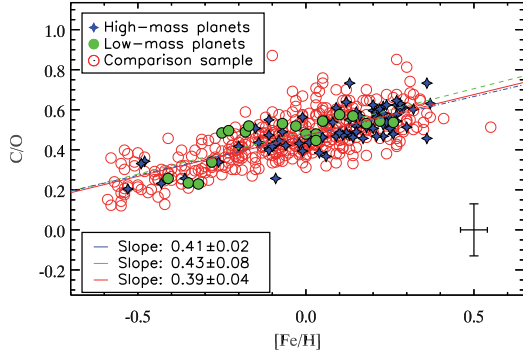


Fig. 1. C/O vs. [Fe/H]. Red open circles refer to single stars while green dots refer to low-mass planet host stars and blue diamonds to high-mass planet-hosts.

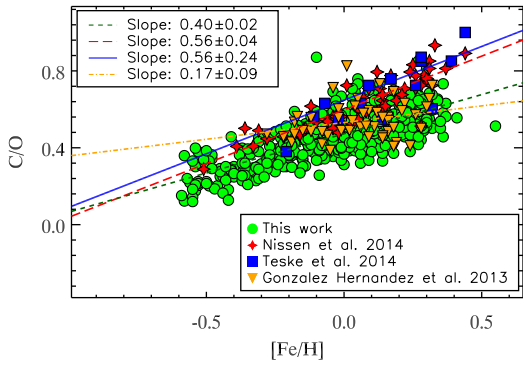


Fig. 2. Comparative C/O vs. [Fe/H]. Green dots show data from our work; red stars show results from [Nissen et al. \(2014\)](#); blue squares from [Teske et al. \(2014\)](#); orange triangles from [González Hernández et al. \(2013\)](#).

dependence on the distance for volatile elements will affect the C/O expected in exoplanetary atmospheres, as volatiles are heavily affected by different distances (or different ice line positions) during the early lifetime of the nebula while planets accrete ([Öberg et al. 2011](#); [Ali-Dib et al. 2014](#); [Brewer et al. 2017](#)).

Figure 1 shows the C/Os derived in this paper as a function of [Fe/H] for these samples; stars with and without planets. We obtain a linear fit for both samples, with very little differences between them. We can see a dependence of C/O on metallicity, in agreement with other works, such as [Nissen et al. \(2014\)](#), [Teske et al. \(2014\)](#) and [Brewer & Fischer \(2016\)](#).

Several authors have studied the C/O ratios in stars with planets (e.g. [Petigura & Marcy 2011](#); [Nissen 2013](#); [Nissen et al. 2014](#); [Teske et al. 2014](#)). In Fig. 2 we can see our results compared with the work of [Nissen et al. \(2014\)](#), [Teske et al. \(2014\)](#), and [González Hernández et al. \(2013\)](#). To make this comparison possible, we scaled the carbon and oxygen abundances presented by these authors to our reference values ($\log N_{\odot}(\text{O}) = 8.71$ and $\log N_{\odot}(\text{C}) = 8.50$). As seen in Fig. 2, there is a good fit at all metallicities between our work and these previous studies.

To test for possible relationships between C/O and the masses of planetary companions, we separated the planet population into two groups: low-mass planets (LMP; with masses less than or equal to $30 M_{\oplus}$) and high-mass planets (HMP; with masses greater than $30 M_{\oplus}$). In those stars which host several planets, the most massive planet in the system was considered in our study. Our sample consists of 19 low-mass and 80 high-mass planet hosts. If we take a closer look at the C/O distribution for the studied samples in Fig. 3, we can see that the planetary samples

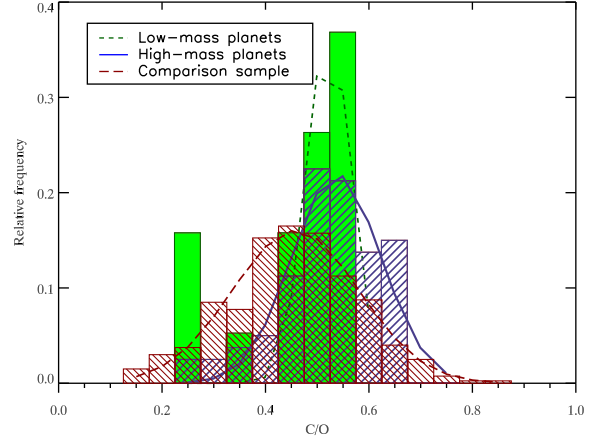


Fig. 3. C/O distributions for stars harbouring low-mass (green) and high-mass (blue) planets. Stars without planets are shown in red.

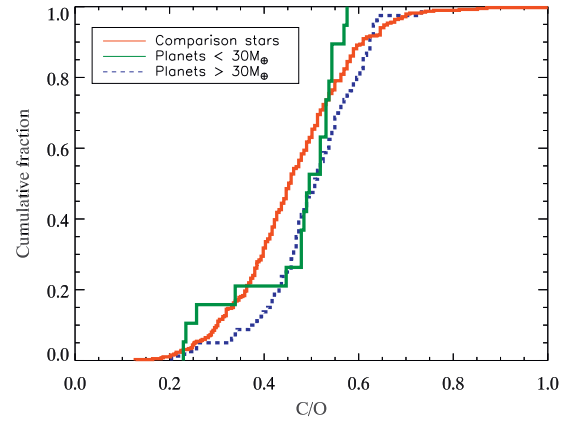


Fig. 4. Cumulative C/O distributions for single stars (red) and stars with planets (low-mass in green and high-mass planets in blue).

exhibit almost the same behaviour, with a small offset, while the single star sample spreads more, with a significant higher FWHM (see Table 2). In our sample, 100% of stars with planets have C/O values lower than 0.8. Average value for the low-mass and high-mass samples are 0.46 ± 0.11 and 0.50 ± 0.10 , respectively. Average value for the single stars sample is 0.45 ± 0.13 . Our stars are slightly carbon poor when compared to the solar reference ($C/O_{\odot} = 0.61$). These results agree, within errors, with those presented in [Nissen et al. \(2014\)](#), [Teske et al. \(2014\)](#), [González Hernández et al. \(2013\)](#).

We can see in Fig. 3 the C/O distributions for single stars and both planetary samples. A cumulative histogram (Fig. 4) shows us that each sample behaves in a different way. We performed a Kolmogorov–Smirnov test (K–S test) to confirm these behaviours. The null hypothesis is rejected at level $\alpha = 0.1$ if our results are higher than $D_{n,n'} = 0.29$ and $D_{n,n'} = 0.15$, for the low-mass and high-mass samples, respectively, following the expression

$$D_{n,n'} > c(\alpha) \sqrt{\frac{n+n'}{nn'}}; c(\alpha = 0.10) = 1.22. \quad (2)$$

We can see in Table 3 that the C/O is above the threshold limit. The probabilities of similarity are 4% and 0% for the low and high-mass samples, respectively, so we can assume that the samples do not come from the same distribution.

Table 2. Statistics for the fitted histograms presented in Figs. 3, 6, and 11.

	Sample	Centre-fit	<i>FWHM</i>
C/O	Single stars	0.45	0.29
	Planets: LMP	0.52	0.10
	Planets: HMP	0.52	0.21
Mg/Si	Single stars	1.11	0.22
	Planets: LMP	1.06	0.25
	Planets: HMP	1.08	0.16
[C/O] _{corr}	Single stars	-0.11	0.25
	Planets: LMP	-0.01	0.11
	Planets: HMP	-0.03	0.17

Notes. The low-mass planets (LMP) and the high-mass planets sample (HMP).

Table 3. K–S test for all the samples.

Sample	C/O	Mg/Si
LMP-NP	0.31	0.16
HMP-NP	0.25	0.12

4.2. Mg/Si

The magnesium and silicon elemental abundance ratio controls the exact composition of silicates that can be found in the planetary companion, as this ratio, along with Fe/Si, does not depend so strongly on the distance to the star as the C/O ratio does (Thiabaud et al. 2015a,b; Dorn et al. 2015).

In Fig. 5 top panel we show Mg/Si ratios as a function of metallicity. As expected, the Mg/Si ratio decreases with [Fe/H], with a similar slope for all the studied sample (see Table 4) We also find a relation between values of Mg/Si and T_{eff} , as shown in the bottom panel of Fig. 5. We obtained slopes and standard deviations for the three studied samples (see Table 4) and, due to the high scatter of the single star sample at T_{eff} higher than 6100 K, we cannot conclude any physical difference. However, as we can see that that slopes and scatter increase, we decided not to use these stars with T_{eff} higher than 6100 K to avoid introducing errors to our analysis.

Given the uncertainty of the implication of NLTE corrections for these hot stars, we will study, from now on, only the sample with $T_{\text{eff}} < 6100$ K. The average value for the low-mass and high-mass samples are 1.15 ± 0.08 and 1.12 ± 0.15 , respectively. The average value for the single stars sample is 1.12 ± 0.12 . These results agree, within errors, with those presented in Brewer et al. (2017).

The distribution of Mg/Si for both planet-host stars and the comparison sample are shown in Fig. 6. We can see that all samples exhibit the same behaviour. In our sample 100% of the low-mass sample have an Mg/Si value of between 1.0 and 2.0 while 85% of the high-mass sample exhibit this behaviour. We also find that none of the low-mass planet hosts have Mg/Si values below 1.0, but 15% of the high-mass sample does. No stars with Mg/Si values greater than 2.0 were found.

Figure 7 shows Mg/Si distributions for single stars and both planetary samples. All samples are concentrated around Mg/Si ~ 1.12 , only 0.05 higher than our solar reference (1.07) and within errors. Statistics for these histograms are shown in Table 2. A cumulative histogram (Fig. 7) shows that each sample

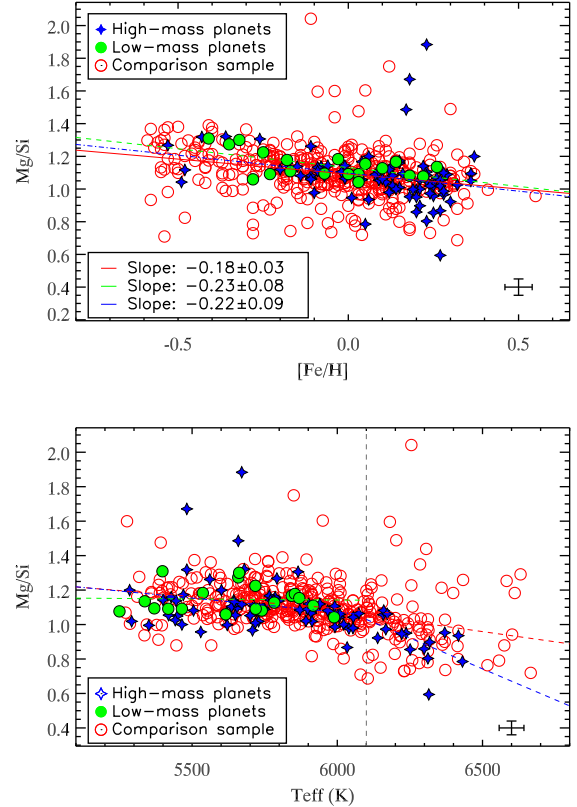


Fig. 5. Mg/Si as a function of [Fe/H] (top panel) and T_{eff} (bottom panel). Red open circles refer to single stars while green dots refer to low-mass planet host stars and blue diamonds to high-mass planet-hosts.

Table 4. Statistics for the three groups studied (Comparison sample, low-mass planets and high-mass planets) for Mg/Si vs. T_{eff} (see Fig. 5, bottom panel).

	Mg/Si vs. T_{eff} (for $T_{\text{eff}} < 6100$)	
	Slope	Slope _{err}
NP	-1.39E-04	0.32E-04
LMP	-1.21E-05	8.98E-05
HMP	-1.63E-04	0.90E-04
	Mg/Si vs. T_{eff} (for $T_{\text{eff}} > 6100$)	
	Slope	Slope _{err}
NP	-2.37E-04	2.54E-04
LMP	–	–
HMP	-7.17E-04	2.97E-04

behaves in the same way. We find no differences between the planetary samples, as all three samples peak around 1.10. The high-mass sample has a broader distribution than the low-mass one, but the limited number of the low-mass sample does not allow us to infer any result other than the similarity between the samples. A similar result can be found in Brewer et al. (2017).

We performed a K–S test to confirm these behaviours between the samples. As we can see in Table 3, right column, we cannot reject the null hypothesis for the any planetary sample, so we have to assume that the samples come from the same distribution.

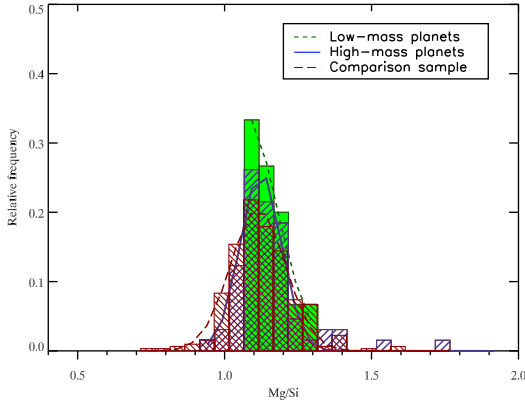


Fig. 6. Mg/Si distributions for stars harbouring low-mass (green) and high-mass (blue) planets. Stars without planets are shown in red.

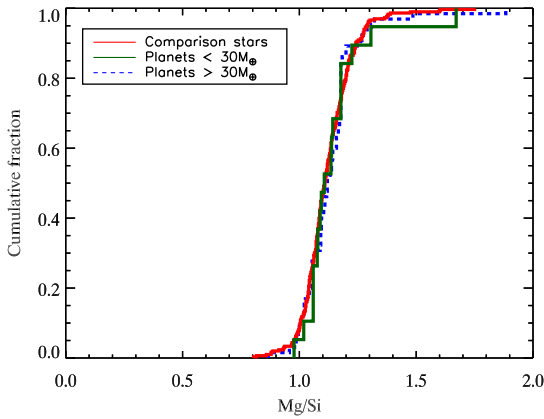


Fig. 7. Cumulative Mg/Si distributions for single stars (red) and stars with planets (low-mass (green) and high-mass planets (blue)).

5. C/O vs. Mg/Si: implications on planet formation

We studied C/O as a function of Mg/Si as a way to study the possible scenario for the formation of planets. In Fig. 8 we see how stars with and without planets are distributed in a C/O against Mg/Si plot. As can be seen, stars with planets, both low-mass and high-mass, are concentrated at C/O values of 0.5–0.6 and Mg/Si values of ~ 1.0 . The solar values of $C/O_{\odot} = 0.61$ and $Mg/Si_{\odot} = 1.07$, derived from the adopted solar values for oxygen, carbon, magnesium, and silicon, are also represented.

As presented in Sect. 4, 100% of the sample with low-mass companions have an Mg/Si value of between 1.0 and 2.0, while 85% of the high-mass companion sample does, which means that Mg is equally distributed between pyroxene and olivine. We also find 15% of high-mass planet hosts with Mg/Si values below 1.0 so Mg and Si will form mainly orthopyroxenes, whereas the remaining Si will take other forms, such as feldspars or olivine. No low-mass companions with Mg/Si values lower than 1.0 were found and no stars with Mg/Si values greater than 2.0 were found either. We highlight the fact that all stars with low-mass companions present $Mg/Si > 1.00$, whereas the high-mass planetary sample can be found for a wide range of Mg/Si values, including $Mg/Si < 1.00$.

Regarding C/O, 100% of stars with planets have C/O values lower than 0.8, meaning that Si will take solid form as SiO_4^{4-} and SiO_2 . Only $\sim 15\%$ of our sample has $C/O < 0.4$ (15 stars). The exact composition will be ruled by the magnesium-to-silicon ratio.

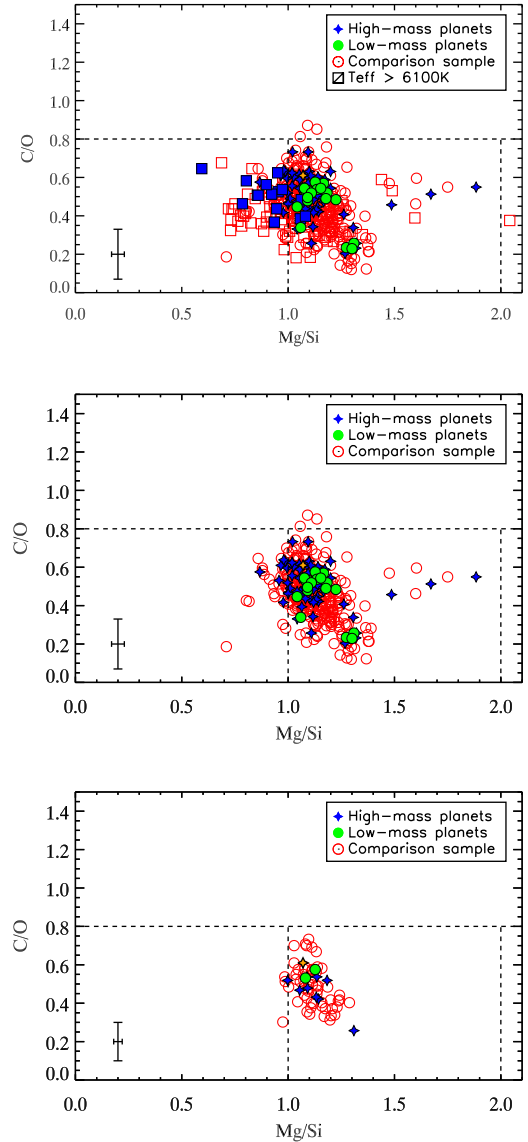


Fig. 8. *Top panel:* C/O vs. Mg/Si. Red circles refer to single stars (400 stars), and green dots refer to stars harbouring planets (99 stars). *Middle panel:* same as the top panel but only for stars with $T_{\text{eff}} < 6100$ K (312 single stars, 19 low-mass planet hosts and 65 high-mass planet hosts). *Bottom panel:* same as top panel but for solar analogues, with $T_{\text{eff}} = T_{\text{eff},\odot} \pm 300$ K, $\log g = \log g_{\odot} \pm 0.2$ dex and $[Fe/H] = [Fe/H]_{\odot} \pm 0.2$ K (58 single stars, 2 low-mass planet hosts and 9 high-mass planet hosts). In all panels, an orange star represents solar values.

Recent models by Carter-Bond et al. (2012), Marboeuf et al. (2014), Thiabaud et al. (2014, 2015a,b) suggest that elemental abundance ratios may suffer great variations when studied in planet host stars and in planetary atmospheres. They proposed that elemental abundance ratios such as Mg/Si and Fe/Si would show similar values in both planet hosts and planetary atmospheres. As for C/O, they proposed large differences between the star and the planets. They suggest that migration plays a key role when forming elemental abundance ratios in planetary atmospheres and the location of planet formation, as the total C/O ratios are governed by ices. Öberg et al. (2011) studied the influence of different snowlines of oxygen and carbon-rich species. They suggest a common region between the H_2O and CO snowlines with giant planetary formation. These snowlines

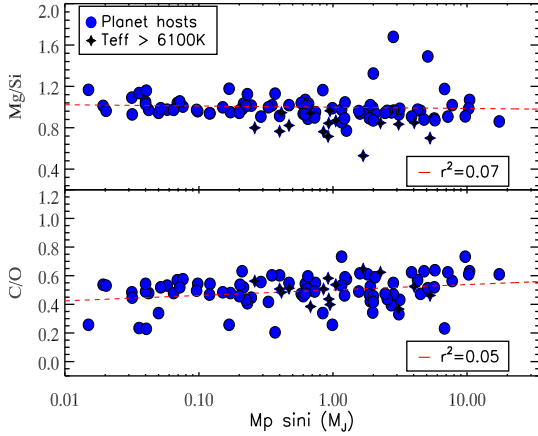


Fig. 9. Mg/Si and C/O elemental abundance ratios as a function of the planetary mass. A correlation for the final sample (stars with $T_{\text{eff}} < 6100$ K) is provided for both sets, C/O and Mg/Si.

and the migration from the original birthplace can affect the abundance of volatiles, but not the abundance of refractory elements, such as Mg, Si, and Fe. This assumption was confirmed for hot-Jupiter hosts by Brewer et al. (2017), where they show that the average planet C/O is super-stellar, but their large uncertainties do not exclude the possibility of the 1:1 relation for the stellar and planetary C/O.

Stars with only low-mass planets are likely to be found in the $1 < \text{Mg/Si} < 1.5$ regime, although mixed with stars with high-mass planets. As seen in Fig. 8, there is a gap for stars with $1.1 < \text{Mg/Si} < 1.3$ and $\text{C/O} < \sim 0.5$. As noted in Sect. 2, stars without planets are likely to be stars with undetected planets. Also, as presented in Sect. 4, there is a dependence in temperature for hotter stars. Since smaller planets will be harder to detect around these hotter stars, our results can be suffering from this effect. More knowledge about these stars and their plausible planetary companion is needed to constrain planetary formation and its relation with elemental abundance ratios more clearly.

6. C/O, Mg/Si, and masses

We studied C/O and Mg/Si as a function of mass of planetary companion (the most massive planet in case of multiple planets). In Fig. 9 we can see a slight dependence on planetary mass, as the slopes are not null (-0.04 for Mg/Si and 0.04 for C/O), but the elemental abundance ratio errors do not allow us to make any further assumptions.

As proposed by Thiabaud et al. (2015b), Mg/Si in stars will give a direct information about the composition of the planet, as no differences are expected between them. Our stellar Mg/Si values can be translated as planetary Mg/Si (see Santos et al. 2015; Dorn et al. 2015).

Regarding C/O, and given the indirect relation between the star and the planet, our results are an estimation of the C/O that could be found in the planet. For example, WASP-12b shows a high C/O, above 1 (Kreidberg et al. 2015), while its host star shows $\text{C/O} = 0.48$ (Teske et al. 2014). Brewer et al. (2017) have proposed that planetary C/O will be super-stellar (while O/H could be sub-stellar) in hot-Jupiters.

7. Galactic trends in [C/O]

Elemental abundance ratios can help us to understand how the planets are formed. In astronomy, solar ratios (e.g. [C/O]) are

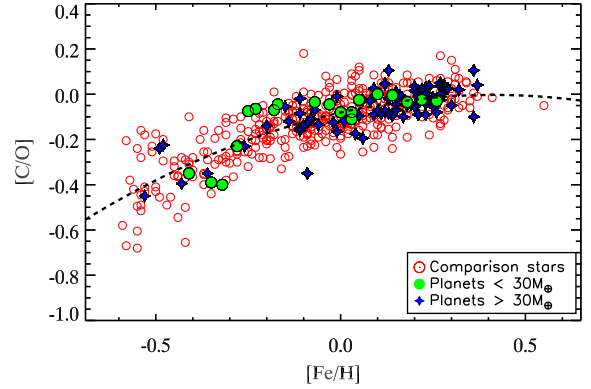


Fig. 10. [C/O] as a function of [Fe/H] for stars with and without detected companions. Trend line provides a quadratic fit to all the data points.

more frequently used, as opposed to absolute ratios (e.g. C/O). However, in order to investigate if the C/O ratios are affected by Galactic chemical evolution (GCE; as Mg/Si is, see Adibekyan et al. 2015), we need to rely on solar ratios ([C/O]), therefore we present in this section a study of [C/O] for our sample.

Several works have already discussed the possible differences in individual elemental abundances and [X/Fe] abundances ratios between stars without detected planets and stars hosting low-mass and high-mass planets (Adibekyan et al. 2012a,c, 2015). As presented in Adibekyan et al. (2015) for a sample of 589 stars, the dependence of [Mg/Si] on metallicity, that is the Galactic evolution of [Mg/Si] ratio, may play an important role in the internal structure and composition of terrestrial planets. Overall, they concluded that stars formed at different times and places in the Galaxy have a different probability of forming low-mass planets, and the composition of the formed planets will also depend on the chemical composition of the environment in which they formed.

The dependence of [C/O] on metallicity, that is, the Galactic evolution of [C/O], may play an important role in the internal structure and composition of high-mass planets (as Mg/Si does for low-mass planets, see Adibekyan et al. 2015). Following this statement, we looked for possible relations between [C/O] and the masses of planetary companions. We separated the planetary population into the same two groups as in the previous analysis (low-mass and high-mass planets).

In Fig. 10 we show the dependence of [C/O] on the metallicity for stars with and without detected planets. This figure shows that C/O has a clear dependence on [Fe/H]. To remove the trend of [C/O] with GCE we fitted all our data points (all stars with and without detected planets) with a quadratic dependence on metallicity and then subtracted the fit. Mean squared deviation for the fit is 0.06^3 . $[\text{C/O}]_{\text{corr}}$ represents the [C/O] after subtracting the fitted values.

Distributions of [C/O] for all the presented sub-samples are shown in Fig. 11. A slight difference can be found between the centres of each Gaussian fitting, but they are within errors (see Table 2). To obtain a clearer picture, we tested the sample using a two Kolmogorov–Smirnov (K–S) test (see Table 5 and Fig. 12). The null hypothesis is rejected at level $\alpha = 0.1$ if our results are higher than $D_{nn'} = 0.29$ and $D_{mm'} = 0.15$, for the low-mass and high-mass samples, respectively. In the first case, [C/O], above the imposed threshold limit, the probabilities of similarity are 4% and 4.09E-03% for the low and high-mass sample, respectively, so we can assume that the samples do not

³ $[\text{C/O}] = -0.45 \times [\text{Fe/H}]^2 + 0.38 \times [\text{Fe/H}] - 0.08$.

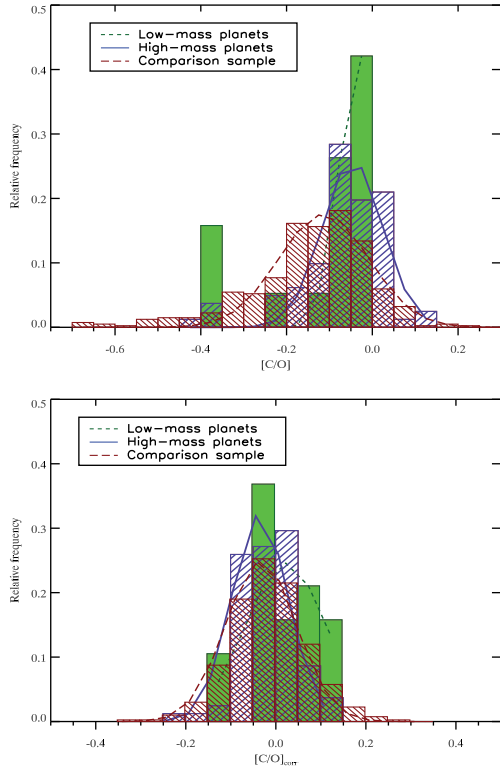


Fig. 11. $[C/O]$ distributions before (*upper panel*) and after ($[C/O]_{\text{corr}}$, *lower panel*) correcting for the Galactic chemical evolution (GCE) effects.

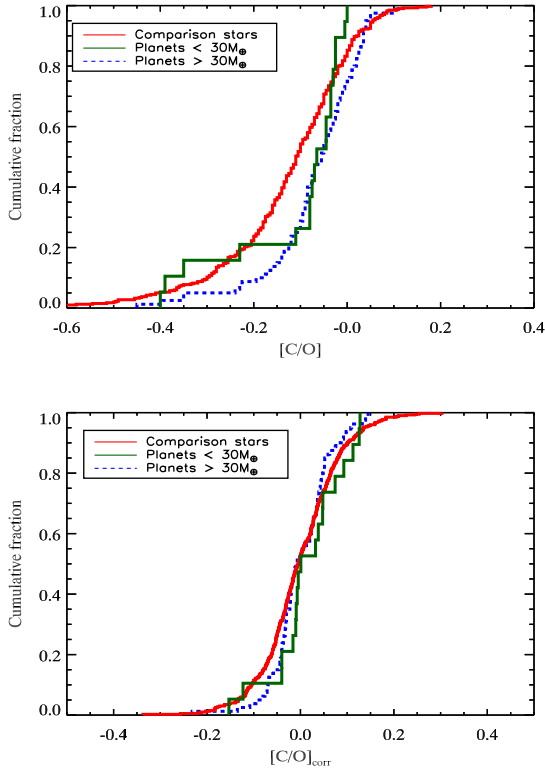


Fig. 12. Cumulative distributions for $[C/O]$, before (*upper panel*) and after (*lower panel*) the GCE correction.

come from the same distribution. In the second case, $[C/O]_{\text{corr}}$, we cannot reject the null hypothesis, but, probabilities are 17%

Table 5. K–S test for GCE and non-GCE corrected samples.

Sample	$[C/O]$	$[C/O]_{\text{corr}}$
LMP-NP	0.31	0.23
HMP-NP	0.28	0.14

and 38%, respectively. Although we cannot assume any conclusion due to the result being below the threshold limit, we can see that probabilities of similarity rises significantly for the high-mass sample. The dependence of $[C/O]$ on metallicity may play an important role in the internal structure and composition of high-mass planets (as Mg/Si does for low-mass planets (see Adibekyan et al. 2015)) but more studies with more data are required to confirm or dismiss this assumption.

8. Summary and conclusions

We present a detailed study of the C/O and Mg/Si elemental abundance ratios for 499 solar-type stars observed with the HARPS high-resolution spectrograph. In our sample, 99 of 499 are planet-hosts and 400 stars have no known planetary companion. All the stars within our sample have effective temperatures between 5250 K and 6666 K, metallicities from -0.59 to 0.55 dex and surface gravities from 3.81 to 4.82 dex.

We separated the planet population into two groups to test for possible relations between elemental abundance ratios and the masses of planetary companions: low-mass planets (LMP; with masses less than or equal to $30 M_{\oplus}$) and high-mass planets (HMP; with masses greater than $30 M_{\oplus}$). All samples show the same distribution in a histogram, with all centre-fit similar within errors. Regarding the planetary sample, we cannot discern the high-mass from the low-mass sample.

We studied the probability of the samples being drawn from the same distribution by applying a K–S test to our samples. For the C/O case, our result suggest no similarity between the samples. For Mg/Si, we cannot reject the null hypothesis, so we have to assume that our samples come from the same distribution. Overall, 99% of our sample present $C/O < 0.8$, while all our confirmed planet host stars present C/O values below 0.8 (with peaks around 0.47), suggesting that the composition of the bulk of the planets should be SiO_4^{4-} and SiO_2 , serving as seeds for Mg silicates. $\sim 15\%$ of our sample has $C/O < 0.4$. Regarding Mg/Si, and after separating our planetary sample in low-mass and high-mass companions, we found that none of our low-mass planet host sample present Mg/Si values lower than one, while 15% of the high-mass sample does, suggesting a composition of pyroxene and feldspars for this sample.

100% of our low-mass sample present Mg/Si values between one and two, so an equal proportion of olivine and pyroxene is expected. 85% of the high-mass sample present these values. These results agree (within the errors and taking into account different solar reference values) with recent studies of C/O and Mg/Si in the solar neighbourhood, such as Brewer & Fischer (2016), as they obtained peaks for distributions at ~ 0.5 for C/O and ~ 1.1 for Mg/Si. Given these results, several different planet compositions could be found in planet hosts that meet these C/O and Mg/Si restrains.

In the last few years, several models have suggested that C/O in planet host stars and planetary atmospheres is not the same, owing to migrations and snowlines, although more observations of atmospheres in transiting exoplanets are required to confirm

these models (Carter-Bond et al. 2012; Öberg et al. 2011; Marboeuf et al. 2014; Thiabaud et al. 2014, 2015a,b).

These ratios give a suggestion of possible planetary abundances. As there is a direct relation between host star and planet abundances for Mg/Si, we can confirm the composition of the planets. Most of our planetary sample (100% of the low-mass and 85% of the high-mass sample) will have pyroxene and olivine as main components, while the other 15% of high-mass companions will have a composition based on orthopyroxene and minerals such as feldspar or olivine.

For C/O, as the elements composing this ratio are sensitive to icelines, the observed planetary values can be up to three-four times the solar value, as recent observations suggest (Brewer et al. 2017). Planetary C/O values can be up to four times the proposed stellar values.

We studied [C/O] and its relation with metallicity (as Mg/Si is affected, see Adibekyan et al. 2015). We do not find a clear relation between high-mass planets and [C/O], but our results suggest that more data is needed to confirm this assumption. Our results for [C/O]_{corr} are below the threshold limit but suggesting a significant increase for the probability of similarity between the high-mass and the comparison star samples.

Acknowledgements. We thank the reviewer for his/her thorough review and highly appreciate the comments and suggestions, which significantly contributed to improving the quality of the publication. J.I.G.H. acknowledges financial support from the Spanish Ministry of Economy and Competitiveness (MINECO) under the 2013 Ramón y Cajal programme MINECO RYC-2013-14875, and the Spanish ministry project MINECO AYA2014-56359-P. V.Zh.A., E.D.M., N.C.S. and S.G.S. acknowledge the support from Fundação para a Ciência e a Tecnologia (FCT) through national funds and from FEDER through COMPETE2020 by the following grants UID/FIS/04434/2013 & POCL-01-0145-FEDER-007672, PTDC/FIS-AST/7073/2014 & POCL-01-0145-FEDER-016880 and PTDC/FIS-AST/1526/2014 & POCL-01-0145-FEDER-016886. V.Zh.A., E.D.M., N.C.S. and S.G.S. also acknowledge the support from FCT through Investigador FCT contracts IF/00650/2015, IF/00849/2015/, IF/00169/2012/CP0150/CT0002 and IF/00028/2014/CP1215/CT0002. This work has made use of the VALD database, operated at Uppsala University, the Institute of Astronomy RAS in Moscow, and the University of Vienna.

References

- Adibekyan, V. Z., Santos, N. C., Sousa, S. G., et al. 2012a, *A&A*, 543, A89
 Adibekyan, V. Z., Sousa, S. G., Santos, N. C., et al. 2012b, *A&A*, 545, A32
 Adibekyan, V. Z., Delgado Mena, E., Sousa, S. G., et al. 2012c, *A&A*, 547, A36
 Adibekyan, V. Z., González Hernández, J. I., Delgado Mena, E., et al. 2014, *A&A*, 564, L15
 Adibekyan, V., Santos, N. C., Figueira, P., et al. 2015, *A&A*, 581, L2
 Adibekyan, V., Gonçalves da Silva, H. M., et al. 2017, *Astrophysics*, 60, 325
 Ali-Dib, M., Mousis, O., Petit, J.-M., & Lunine, J. I. 2014, *ApJ*, 785, 125
 Anders, E., & Grevesse, N. 1989, *Geochim. Cosmochim. Acta*, 53, 197
 Bergemann, M., Collet, R., Amarsi, A. M., et al. 2017, *ApJ*, 847, 15
 Bertran de Lis, S., Delgado Mena, E., Adibekyan, V. Z., Santos, N. C., & Sousa, S. G. 2015, *A&A*, 576, A89
 Bond, J. C., O'Brien, D. P., & Laretta, D. S. 2010a, *ApJ*, 715, 1050
 Bond, J. C., Laretta, D. S., & O'Brien, D. P. 2010b, *Icarus*, 205, 321
 Brewer, J. M., & Fischer, D. A. 2016, *ApJ*, 831, 20
 Brewer, J. M., Fischer, D. A., & Madhusudhan, N. 2017, *AJ*, 153, 83
 Caffau, E., Ludwig, H.-G., Steffen, M., et al. 2008, *A&A*, 488, 1031
 Caffau, E., Ludwig, H.-G., Bonifacio, P., et al. 2010, *A&A*, 514, A92
 Carter-Bond, J. C., O'Brien, D. P., & Raymond, S. N. 2012, *ApJ*, 760, 44
 Delgado Mena, E., Israelian, G., González Hernández, J. I., et al. 2010, *ApJ*, 725, 2349
 Dorn, C., Khan, A., Heng, K., et al. 2015, *A&A*, 577, A83
 Elser, S., Meyer, M. R., & Moore, B. 2012, *Icarus*, 221, 859
 Faria, J. P., Santos, N. C., Figueira, P., et al. 2016, *A&A*, 589, A25
 Figueira, P., Santos, N. C., Pepe, F., Lovis, C., & Nardetto, N. 2013, *A&A*, 557, A93
 Fischer, D. A., & Valenti, J. 2005, *ApJ*, 622, 1102
 Gonzalez, G. 1997, *MNRAS*, 285, 403
 Gonzalez, G. 2006, *PASP*, 118, 1494
 González Hernández, J. I., Israelian, G., Santos, N. C., et al. 2010, *ApJ*, 720, 1592
 González Hernández, J. I., Delgado-Mena, E., Sousa, S. G., et al. 2013, *A&A*, 552, A6
 Haywood, M. 2008, *A&A*, 482, 673
 Haywood, M. 2009, *ApJ*, 698, L1
 Konopacky, Q. M., Barman, T. S., Macintosh, B. A., & Marois, C. 2013, *Science*, 339, 1398
 Kreidberg, L., Line, M. R., Bean, J. L., et al. 2015, *ApJ*, 814, 66
 Lo Curto, G., Mayor, M., Benz, W., et al. 2010, *A&A*, 512, A48
 Lodders, K. 2003, *ApJ*, 591, 1220
 Madhusudhan, N., Lee, K. K. M., & Mousis, O. 2012, *ApJ*, 759, L40
 Marboeuf, U., Thiabaud, A., Alibert, Y., Cabral, N., & Benz, W. 2014, *A&A*, 570, A36
 Mayor, M., Pepe, F., Queloz, D., et al. 2003, *The Messenger*, 114, 20
 Mayor, M., Marmier, M., Lovis, C., et al. 2011, ArXiv e-prints [arXiv: 1109.2497]
 Morgan, J. W., & Anders, E. 1980, *Proc. Natl. Acad. Sci.*, 77, 6973
 Moses, J. I., Madhusudhan, N., Visscher, C., & Freedman, R. S. 2013, *ApJ*, 763, 25
 Nissen, P. E. 2013, *A&A*, 552, A73
 Nissen, P. E., Chen, Y. Q., Carigi, L., Schuster, W. J., & Zhao, G. 2014, *A&A*, 568, A25
 Öberg, K. I., Murray-Clay, R., & Bergin, E. A. 2011, *ApJ*, 743, L16
 Petigura, E. A., & Marcy, G. W. 2011, *ApJ*, 735, 41
 Portinari, L., Chiosi, C., & Bressan, A. 1998, *A&A*, 334, 505
 Santos, N. C., Israelian, G., & Mayor, M. 2001, *A&A*, 373, 999
 Santos, N. C., Israelian, G., & Mayor, M. 2004, *A&A*, 415, 1153
 Santos, N. C., Mayor, M., Bonfils, X., et al. 2011, *A&A*, 526, A112
 Santos, N. C., Adibekyan, V., Mordasini, C., et al. 2015, *A&A*, 580, L13
 Sousa, S. G., Santos, N. C., Mayor, M., et al. 2008, *A&A*, 487, 373
 Sousa, S. G., Santos, N. C., Israelian, G., et al. 2011a, *A&A*, 526, A99
 Sousa, S. G., Santos, N. C., Israelian, G., Mayor, M., & Udry, S. 2011b, *A&A*, 533, A141
 Suárez-Andrés, L., Israelian, G., González Hernández, J. I., et al. 2016, *A&A*, 591, A69
 Suárez-Andrés, L., Israelian, G., González Hernández, J. I., et al. 2017, *A&A*, 599, A96
 Teske, J. K., Cunha, K., Smith, V. V., Schuler, S. C., & Griffith, C. A. 2014, *ApJ*, 788, 39
 Thiabaud, A., Marboeuf, U., Alibert, Y., et al. 2014, *A&A*, 562, A27
 Thiabaud, A., Marboeuf, U., Alibert, Y., Leya, I., & Mezger, K. 2015a, *A&A*, 574, A138
 Thiabaud, A., Marboeuf, U., Alibert, Y., Leya, I., & Mezger, K. 2015b, *A&A*, 580, A30
 Tsantaki, M., Sousa, S. G., Adibekyan, V. Z., et al. 2013, *A&A*, 555, A150